Check for updates

Theoretical design of bis-azole derivatives for energetic compounds†

Keyu Pu,[a] Linyuan Wang, [ID] *[a] Jian Liu[b] and Kai Zhong[b]

Bis-azole derivatives are a new class of energetic materials with features that include high nitrogen content, high heat of formation (HOF), high detonation performance and insensitivity to external stimuli. In this paper, 599 new bis-azole compounds were designed in a high-throughput fashion using bis-azole molecules of high density and high thermal decomposition temperature as the basic structure, and high energy groups such as nitro (–NO_2) and amino groups (–NH_2) as substituents. The molecular geometry optimization and vibration frequency analysis were performed using the DFT-B3LYP/6-311++G(d,p) method. The calculation results show that none of bis-azole derivatives exhibit a virtual frequency. Additionally, the density, heat of formation and characteristic height (h_{50}) of the above compounds were obtained. Detonation performances were predicted by the Kamlet–Jacobs equations, and their structures and performances were studied. Furthermore, correlations between the performance parameters and the parent structure of the molecule, the number of substituting group and configuration were summarized, revealing promising potential candidates for high-energy density materials (HEDMs).

1 Introduction

Energetic materials such as explosives, propellants and pyrotechnics play a vital role in the fields of military, defense, aerospace technology and modern civilization. Recently, novel insensitive HEDMs have become a target for further research and development.[1–3] There is a conflict between energy and stability, and the increase in energy is often accompanied by an increase in sensitivity, which poses a challenge for balancing both parameters.[4] In recent years, heterocyclic molecules have been introduced into the molecular design due to their advantages of increasing heat resistance and decreasing sensitivity.[5] Nanjing University of Science and Technology (NUST) has carried out the molecular design of novel high-energy nitrogen heterocyclic compounds[6] with computer technology, which has potential application value in the field of propellants and explosives. The azole ring compounds have become a research hotspot because they have high nitrogen content, high heat of formation, high gas production and produce clean detonation products.[7–13] Previously, researchers synthesized various bis-azoles compounds by changing substituents. The synthesis of energetic materials is dangerous, and the characterization is difficult, so theoretical prediction becomes the first choice. This method not only evaluates the performance in advance and

reveals the relationship between structures and properties, but also provides guidance for experimental synthesis and reduction of the experimental blindness.[14–16]

In addition to the advantages of traditional azole compounds like high nitrogen content and high heat of formation, the bis-azole compounds also have higher density and lower sensitivity. Compared to traditional nitramines, the bis-azole compounds have more advantages including more convenient control of reaction processes and less environmental impact. Therefore, it is expected to be widely used in production of low-signature propellant, low-smoke fireworks and new explosives.[17] In this paper, 599 kinds of nitro-containing compounds were generated by the automatic assembly of the skeleton and functional groups, with each high-energy bis-azole ring as the skeleton, –NH_2 as the stabilizing group and –NO_2 as the detonating group.[18] Compounds were divided into four groups (A–D) according to the skeleton type. The B3LYP/6-311++G(d,p) level of the density functional theory (DFT)[19–21] has been applied to study the molecular geometry, density, heat of formation, detonation property and stability of the compounds. Furthermore, the relationship between structure and property was analyzed, and seven compounds meeting the requirements (*i.e.* high energy and low sensitivity) were selected as potential novel HEDMs.

2 Computational methods

A series of studies by Xiao Heming *et al.*[22–24] on systems containing C, H, O, N and other elements show that the B3LYP method can provide reliable geometric structures and other

[a]School of Chemistry and Chemical Engineering, Southwest Petroleum University, Chengdu 610500, China. E-mail: vbgr5808062c@163.com

[b]Institute of Chemical Materials, CAEP, Mianyang 621999, China

† Electronic supplementary information (ESI) available. See DOI: 10.1039/d0ra00385a

information in the study of energetic materials. Molecular geometries of the bis-azole derivatives were fully optimized at the B3LYP/6-311++G(d,p) level. The vibration frequency analysis showed that none of the optimized structures exhibited imaginary frequencies, and when all optimized structures corresponded to the local energy minimum points on the respective potential energy surfaces, the stable structures were obtained. DFT combined with the atomization scheme[25–28] is used to predict heat of formation, and the principle of the atomization scheme is as follows:

$$C_aH_bO_cN_d(g) \rightarrow aC(g) + bH(g) + cO(g) + dN(g) \quad (1)$$
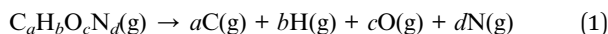
That is, the molecule is decomposed into atoms, and the formula for heat of formation ΔH_{298} at 298 K is

$$\Delta H_{298} = \sum \Delta H_{f,p} - \sum \Delta H_{f,R} = a\Delta H_{f,C} + b\Delta H_{f,H} + c\Delta H_{f,O} + d\Delta H_{f,N} - \Delta H_{f,C_aH_bO_cN_d} \quad (2)$$

where $\Delta H_{f,p}$ and $\Delta H_{f,R}$ are the standard heat of formation (298 K) of products and reactants, $\Delta H_{f,C}$, $\Delta H_{f,H}$, $\Delta H_{f,O}$ and $\Delta H_{f,N}$ are the standard heat of formation (298 K) of C, H, O and N atoms, which can be obtained from the manual, and $\Delta H_{f,C_aH_bO_cN_d}$ is the standard heat of formation (298 K) of the $C_aH_bO_cN_d$ molecule, which needs to be obtained through calculation.

Additionally,

$$\Delta H_{298} = \Delta E_{298} + \Delta(pV) = \Delta E_0 + \Delta E_{ZPE} + \Delta nRT = E_{0,C} + E_{0,H} + E_{0,O} + E_{0,N} - E_{0,C_aH_bO_cN_d} - E_{ZPE,C_aH_bO_cN_d} - \Delta E_{T,C_aH_bO_cN_d} + \Delta nRT \quad (3)$$

where $E_{0,C}$, $E_{0,H}$, $E_{0,O}$, $E_{0,N}$ and $E_{0,C_aH_bO_cN_d}$ are the calculated total energy (0 K) of C, H, O and N atoms and $C_aH_bO_cN_d$ molecule, respectively. $E_{ZPE,C_aH_bO_cN_d}$ and $\Delta E_{T,C_aH_bO_cN_d}$ are the zero point energy and thermal correction value of molecule $C_aH_bO_cN_d$, which can be obtained from vibration analysis thermodynamic data, and the E_{ZPE} and ΔE_T are zero for atoms. The term Δn is the difference value of the amount of substance between gaseous products and reactants, R is the gas constant, 8.314 J mol^{-1} K^{-1}, and T is the absolute temperature, K. According to the above atomization scheme, gas phase heat of formation is obtained, and the solid phase heat of formation is obtained by subtracting the sublimation heat from the gas phase heat of formation of each compound. The sublimation heat of each compound can be obtained by reading the Gaussian output file.

The characteristic height (h_{50}) can be computed using the following formula, which evaluates the impact sensitivity and stability of energetic compounds,[29,30] as suggested by Cao:[31]

$$h_{50} = 0.1296 + 98.64Q_{NO_2}^2 - 0.03405OB_{100} \quad (4)$$

where Q_{NO_2} is the net Mulliken charge of the nitro group, and OB_{100} is the oxygen balance. In general, the higher the negative charge on the nitro group, the more stable the compound. The following equation was used to calculated OB_{100}:

$$OB_{100} = \frac{100(2n_O - n_H - 2n_C - 2n_{COO})}{M} \quad (5)$$

where n_O, n_H and n_C are the numbers of O, H and C atoms in the molecule, n_{COO} represents the number of carboxyl groups, and M is the molecular weight.

Density directly affects the detonation performance.[32] In this paper, the density is calculated by $\rho = 0.9183\left(\dfrac{M}{V_m}\right) + 0.0028(\upsilon\sigma_{tot}^2) + 0.0443$ of Politzer's method,[33,34] where M is the molecular mass, V_m is the molecular van der Waals volume and $\upsilon\sigma_{tot}^2$ reflects the characteristics of the molecules surface electrostatic potentials. Based on the Monte-Carlo method,[35,36] V_m is the volume to be defined as the space within a contour of $0.001e$ bohr^{-3} (a.u.) density under stable structures. This method for calculating V_m has been successfully applied to the high nitrogen compounds.[37] The calculation was performed using the Gaussian 09 and Multiwfn programs.[38,39]

Detonation performance is an important indicator to evaluate the quality of energetic materials. For C-, H-, O- and N-series explosives, the widely used semiempirical Kamlet–Jacobs equation[40,41] was used to predict the detonation performance:

$$D = \varphi^{1/2}(1.011 + 1.312\rho) \quad (6)$$

$$\varphi = N\bar{M}^{1/2}Q^{1/2} \quad (7)$$

$$p = 1.558\varphi\rho^2 \quad (8)$$

where ρ is the density (g cm^{-3}), D is the detonation velocity (km s^{-1}), p is the detonation pressure (GPa), φ is the explosive characteristic value, N is the amount of gaseous detonation product per gram of explosive (mol g^{-1}), $\bar{M}$ is the average molar mass of gaseous detonation products (g mol^{-1}), Q is the detonation chemical energy per gram of explosive (maximum detonation heat per unit mass), J g^{-1}. The term $Q = -\Delta H_{f,298}$, which is the heat of formation. Combined with the heat of formation obtained from the atomization scheme, Q was obtained by using a previously reported method in.[23] From the above equation, it can be seen that the impact of the value of $Q(-\Delta H_{f,298})$ on D and p is insignificant, while ρ great influences the estimation of D and p. Previous studies have shown that[42–45] the use of the K–J equation to predict detonation performance of high nitrogen compounds is reliable.

All of the above calculation methods and rationales were developed using B3LYP/6-311++G(d,p), and the calculation was performed using the Gaussian 09 quantum chemistry program[46] and quantum chemistry Multiwfn program. Additionally, all DFT calculations were performed on the high-throughput computing platform EM-studio1.0 for energetic materials, and the convergence precision is the default value of the program.

3 Results and discussion

Through the use of a high-throughput computing platform, 599 compounds were designed. The molecular structures of A and C series derivatives are listed in Table 1, and the molecular

Table 1 Molecular structures of each series of bis-azole derivatives[a]

A

A1: R_1 = H, R_2 = NO_2
A2: R_1 = NH_2, R_2 = NO_2
A3: $R_{1,2}$ = NO_2

C

C1: R_1 = H, R_2 = NO_2
C2: R_1 = NH_2, R_2 = NO_2
C3: $R_{1,2}$ = NO_2

B

B1: $R_{1,2,4}$ = H, R_3 = NO_2
B2: $R_{1,2,3}$ = H, R_4 = NO_2
B3: $R_{1,2}$ = H, $R_{3,4}$ = NO_2
B4: $R_{1,3}$ = H, $R_{2,4}$ = NO_2
B5: $R_{1,4}$ = H, $R_{2,3}$ = NO_2
B6: $R_{2,3}$ = H, $R_{1,4}$ = NO_2
B7: R_1 = H, R_3 = NH_2, $R_{2,4}$ = NO_2
B8: R_2 = H, R_1 = NH_2, $R_{3,4}$ = NO_2
B9: R_1 = H, R_2 = NH_2, $R_{3,4}$ = NO_2
B10: R_3 = H, R_1 = NH_2, $R_{2,4}$ = NO_2
B11: R_1 = H, R_4 = NH_2, $R_{2,3}$ = NO_2
B12: R_2 = H, R_3 = NH_2, $R_{1,4}$ = NO_2
B13: $R_{2,3}$ = NH_2, $R_{1,4}$ = NO_2
B14: $R_{1,3}$ = NH_2, $R_{2,4}$ = NO_2
B15: $R_{1,4}$ = NH_2, $R_{2,3}$ = NO_2
B16: $R_{1,2}$ = NH_2, $R_{3,4}$ = NO_2
B17: R_2 = NH_2, $R_{1,3,4}$ = NO_2
B18: R_2 = H, $R_{1,3,4}$ = NO_2
B19: R_1 = H, $R_{2,3,4}$ = NO_2
B20: R_1 = NH_2, $R_{2,3,4}$ = NO_2
B21: $R_{1,2,3,4}$ = NO_2

D

D6: $R_{4,6}$ = H, $R_{1,2,3}$ = NH_2, R_5 = NO_2
D7: $R_{1,3,6}$ = H, $R_{4,5}$ = NH_2, R_2 = NO_2
D8: $R_{1,3}$ = H, $R_{4,5,6}$ = NH_2, R_2 = NO_2
D31: $R_{1,3,5}$ = H, $R_{2,6}$ = NH_2, R_4 = NO_2
D32: $R_{2,3,4,6}$ = H, R_1 = NH_2, R_5 = NO_2
D33: $R_{1,2,3,4,6}$ = H, R_5 = NO_2
D34: $R_{2,5,6}$ = H, $R_{1,3}$ = NH_2, R_4 = NO_2
D35: $R_{2,3,4}$ = H, $R_{5,6}$ = NH_2, R_1 = NO_2
D120: R_2 = H, $R_{1,3,4,5}$ = NH_2, R_6 = NO_2
D121: R_1 = H, $R_{2,3,4,5}$ = NH_2, R_6 = NO_2
D122: $R_{1,2,3,4,5}$ = NH_2, R_6 = NO_2
D123: $R_{2,4,6}$ = H, $R_{1,5}$ = NH_2, R_3 = NO_2
D124: $R_{2,4}$ = H, $R_{1,5,6}$ = NH_2, R_3 = NO_2
D125: R_2 = H, $R_{1,4,5,6}$ = NH_2, R_3 = NO_2
D146: $R_{1,2,4,5}$ = H, R_6 = NH_2, R_3 = NO_2
D147: $R_{1,2,5}$ = H, $R_{4,6}$ = NH_2, R_3 = NO_2
D148: $R_{1,4,5,6}$ = H, R_2 = NH_2, R_3 = NO_2
D152: R_2 = H, $R_{1,4,5}$ = NH_2, $R_{3,6}$ = NO_2
D153: R_4 = H, $R_{1,5,6}$ = NH_2, $R_{2,3}$ = NO_2
D154: $R_{4,6}$ = H, $R_{1,5}$ = NH_2, $R_{2,3}$ = NO_2
D176: $R_{1,4,5}$ = H, $R_{2,3,6}$ = NO_2
D177: $R_{4,5}$ = H, R_1 = NH_2, $R_{2,3,6}$ = NO_2
D178: R_5 = H, $R_{1,4}$ = NH_2, $R_{2,3,6}$ = NO_2
D183: $R_{5,6}$ = H, $R_{1,2,3,4}$ = NO_2
D237: R_5 = H, $R_{1,2,3,4,6}$ = NO_2
D238: $R_{1,2,3,4,5,6}$ = NO_2

[a] R_1 = H indicates that the R1 substitution site is H, $R_{1,2}$ = H indicates that R1 and R2 substitution sites are H, and the rest are analogous.

structures of partial derivatives of B and D series are listed in Table 1, representing and illustrating the structure and performance rules of B and D series. The molecular structures of all designed derivatives of the B and D series are listed (see Tables S1 and S4 in ESI†).

3.1 Heats of formation

The heat of formation, as the basic thermodynamic property, is an indication of energy level and an important parameter to measure detonation performance. Whether it is to calculate the detonation velocity and detonation pressure of explosives and powders or the specific impulse of propellants, heat of formation occupies a considerable weight in the formula.

Fig. 1 compares the heat of formation of the designed 599 derivatives. In the skeleton of the A series, the O on the isofurazan is replaced by N to obtain the skeleton of the B series. Compared with the A series, the heat of formation of the B series is significantly improved, which indicates that the heat of formation increases with the increase of the nitrogen content, and that the skeleton of the B series is energetic and preferable to that of the A series. It is known from Fig. 1 that the heat of formation of all derivatives are higher than that of the
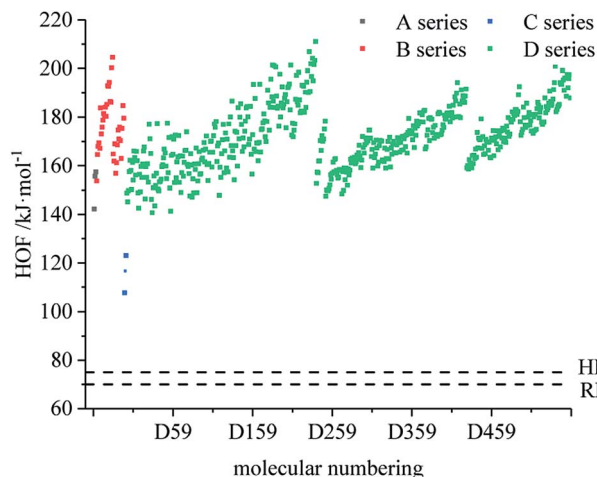
Fig. 1 Comparison of the HOF of each series of bis-azole derivatives.

Fig. 2 The relationship between the HOF and substitution sites (D series).

traditional energetic materials 1,3,5-trinitro-1,3,5-triazinane (RDX) and 1,3,5,7-tetranitro-1,3,5,7-tetrazocane (HMX). All derivatives exhibit high heat of formation (HOF) values. Therefore, the derivatives can be considered endothermic compounds and possess one of the basic conditions of HEDC. The high HOF values of all derivatives are consistent with previous reports, and high nitrogen heterocyclic energetic compounds have high HOF.[47,48] From the perspective of HOF, the application prospects of B and D series are better.

Table 2 shows the heats of formation of partial derivatives, and the heats of formation of all design derivatives of B and D series are presented (see Tables S2 and S5 in ESI†). When the B series substituents are two $-NO_2$ and two $-NH_2$ groups, the HOF of each compound increases in the order of B13 < B14 < B16 < B15. This may be because the reduction of the distance between $-NO_2$ in compounds B13, B14, B16 and B15 leads to the enhancement of steric hindrance effect, thus increasing the HOF of the compound. It indicates that when designing compounds, we can appropriately reduce the distance between $-NO_2$ so as to increase the compound energy. However, when the B series substituents are two $-NO_2$ and one $-NH_2$, the HOF of each compound is: B7 < B8 < B9 < B11 < B10 < B12. Compound B12 has a symmetrical distribution of $-NO_2$ and all

the C and N atoms in the molecule are basically on the same plane. The molecule has a stable geometric configuration, so the molecule has larger conjugation and higher HOF. Meanwhile, when the D series contains one $-NO_2$, the derivatives are D1–D151 and D239–D250. In this case, the $-NO_2$ substitution site of the compound with higher HOF is basically on the carbon atom of the diazole ring (R_3), especially the compounds D131, D133, D141, D143, D144, D150, and D151 have high HOF. It suggests that we can look for high-energy compounds in D series derivatives with $-NO_2$ at the R_3 substitution site. The relationship between the HOF and the substitution site of the D series is shown in Fig. 2. An average HOF of all compounds in the D series that possess an $-NO_2$ group at a certain substitution site (such as R_1) is determined, which is the HOF value corresponding to this substitution site (such as R_1) on the NO_2 line in the figure, and we repeat the above steps for the rest of substitution sites. Similarly, we repeat the above steps to obtain the NH_2 line and the H line when the substituents are NH_2 and H, as shown in Fig. 2. It is known from the figure that when the D series contains one $-NO_2$ group, $-NO_2$ of compounds with higher HOF is basically substituted at R_3, and $-NO_2$ contributes

Table 2 Calculated heats of formation (HOFs) of each series of bis-azole derivatives[a]

Comp.	HOF	Comp.	HOF	Comp.	HOF	Comp.	HOF	Comp.	HOF	Comp.	HOF
A1	142.2	B9	178.8	B20	200.3	D34	151			D152	184.3
A2	155.6	B10	181.5	B21	204.6	D35	155.7			D153	180.1
A3	157.4	B11	180.3	C1	107.7	D120	164.9			D154	168.7
B1	153.7	B12	184.2	C2	116.7	D121	170.7			D176	169.9
B2	164.6	B13	180.3	C3	123.1	D122	177			D177	178.2
B3	167.9	B14	185.3	D6	158	D123	157.1			D178	191.1
B4	169.4	B15	192.9	D7	150.2	D124	166.1			D183	188.4
B5	167.1	B16	192.7	D8	161.4	D125	173.5			D237	203.3
B6	183.8	B17	194.3	D31	165	D146	165.9			D238	211.1
B7	173.1	B18	186.5	D32	146.2	D147	171.4				
B8	175.9	B19	186.2	D33	140.7	D148	167.7				

[a] HOFs (kJ mol^{-1}).
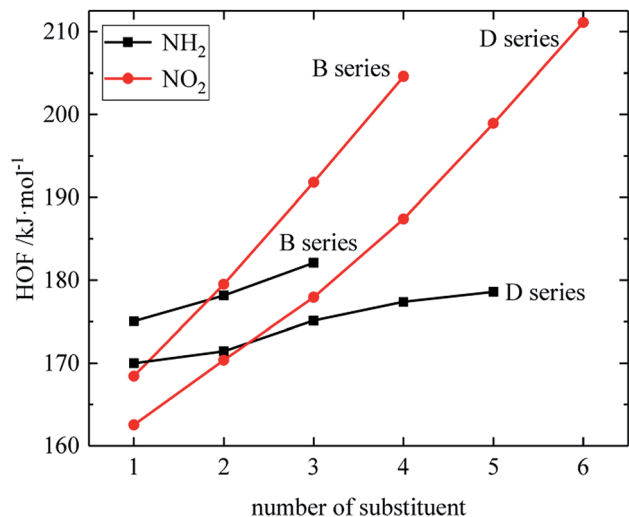
Fig. 3 The relationship between the HOF and number of substituent (B, D series).

Table 3 Calculated h_{50} values of each series of bis-azole derivatives[a]

Comp.	h_{50}	Comp.	h_{50}	Comp.	h_{50}	Comp.	h_{50}	Comp.	h_{50}
A1	297	B9	105	B20	41	D34	42	D152	478
A2	297	B10	75	B21	41	D35	42	D153	482
A3	291	B11	28	C1	216	D120	940	D154	490
B1	43	B12	253	C2	217	D121	952	D176	293
B2	215	B13	269	C3	204	D122	958	D177	328
B3	51	B14	66	D6	65	D123	520	D178	414
B4	93	B15	23	D7	593	D124	524	D183	102
B5	27	B16	70	D8	602	D125	516	D237	116
B6	209	B17	79	D31	41	D146	332	D238	104
B7	84	B18	57	D32	41	D147	424		
B8	45	B19	40	D33	42	D148	343		

[a] h_{50} (cm).

more to the HOF than –NH$_2$. So when designing compounds, we can appropriately introduce multiple –NO$_2$ to improve the HOF of compounds.

The relationship between the HOF of B and D series and the number of substituents is shown in Fig. 3. The relationship between the contributions of different energetic groups to the HOF is –NO$_2$ > –NH$_2$, and the HOF of B and D series increases as the number of –NH$_2$ or –NO$_2$ increases. It can be seen that in each series of derivatives, the influence of substituents on the HOF of the compounds is consistent. Table 2 also shows that the HOF of A and C series increases with the increase of –NO$_2$ number; among the four series, each compound in which all substituents are –NO$_2$ has the highest HOF in the corresponding respective series of compounds. This is because on the one hand, the introduction of –NO$_2$ increases the energy, and on the other hand, the enhancement of the steric hindrance effect of –NO$_2$ also contributes to the energy increase.
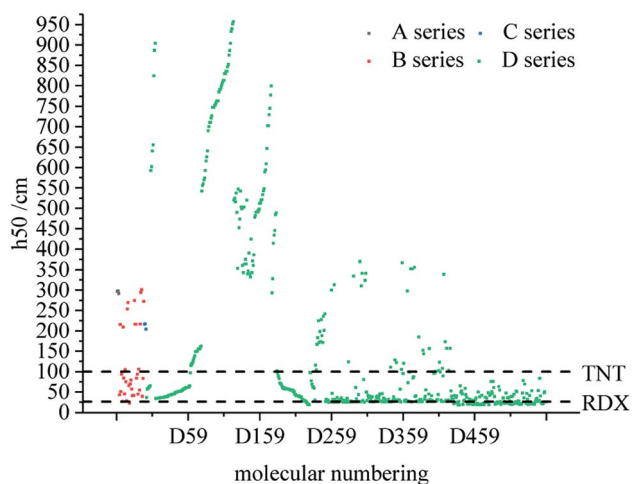
3.2 Sensitivity

The characteristic height (h_{50}) is the height at which the sample is impacted by a given mass and there is 50% probability of causing an explosion. The h_{50} has been calculated to reflect the impact sensitivity and stability of the designed compounds in this work. The larger h_{50}, the more stable the compound.

Fig. 4 compares the h_{50} values of all derivatives. Each series has a compound with a higher h_{50} value than that of TNT (100 cm),[49] which indicates that these series have low sensitivity and good stability. The h_{50} values of all series of derivatives lie in the range of 18–958 cm, which are higher than the h_{50} value (12 cm)[50] of CL-20. Moreover, the h_{50} value of D series derivatives tends to be higher, indicating that this skeleton of D series may be more stable.

Table 3 shows the h_{50} values of partial derivatives. The h_{50} values of all design derivatives of B and D series are presented (see Tables S2 and S5 in ESI†), and the oxygen balance (OB$_{100}$) and nitro group charge (Q_{NO_2}) of all derivatives of the B and D series are listed (see Tables S3 and S6 in ESI†). When the B series contains three –NO$_2$, the h_{50} value of the compound in which substitution sites of –NO$_2$ are adjacent is smaller than that of the isomeride. This behavior can be found in compounds B17 and B20, as well as B18 and B19. Among these compounds, B17 has a higher h_{50} value than B20 (B17 is more stable than B20), and B18 is less sensitive to external stimuli than B19 because the presence of N–NO$_2$ groups or the decrease of the distance between –NO$_2$ in B19 and B20 increases the sensitivity. When the substituents of the B series are one –NO$_2$ and three H, the h_{50} value of each compound is: B2 > B1. The compound B2 has a C–NO$_2$ structure, and the compound B1 has an N–NO$_2$ structure. The h_{50} value of the compound that is substituted at the carbon atom by –NO$_2$ is higher than that of the compound that is substituted at the nitrogen atom by –NO$_2$, so B2 has a higher h_{50} value and lower sensitivity. Additionally, when the B series contains two –NO$_2$ groups, the h_{50} value of each compound decreases in the order of B13, B12, B6, B9, B4, B7, B10, B16, B14, B3, B8, B11, B5 and B15, and the number of N–NO$_2$ increases. These results show that the sensitivity increases as the number of N–NO$_2$ groups increases. The h_{50} values of compounds B6, B12 and B13 are large because the
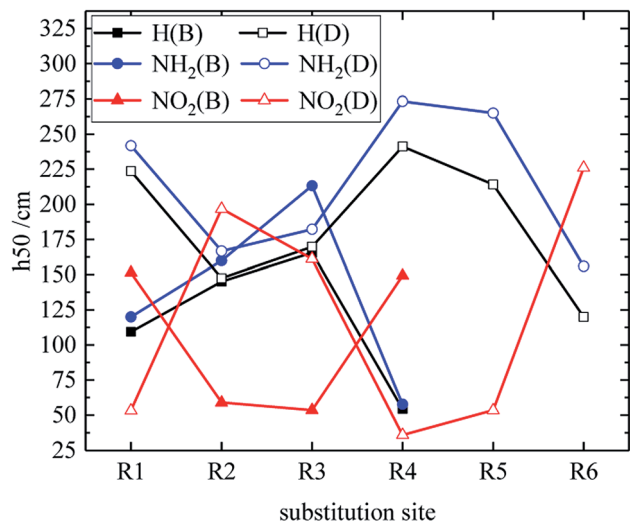

Fig. 4 Comparison of the h_{50} of each series of bis-azole derivatives.

Fig. 5 The relationship between the h_{50} and substitution sites (B, D series).

Fig. 6 The relationship between the h_{50} and number of substituent (B, D series).

–NO$_2$ distribution of these compounds is symmetrical, so the molecules have stable geometric configurations and low sensitivities. Meanwhile, when the D series contains one –NO$_2$, the derivatives are D1–D151 and D239–D250. The –NO$_2$ of a compound with $h_{50} \leq 241$ cm is substituted on nitrogen (D1–D6, D14–D77 and D239–D250), the –NO$_2$ of a compound with $h_{50} > 241$ cm is substituted on carbon (D7–D13, D78–D151). It can be seen that C–NO$_2$ has lower energy and is more stable than N–NO$_2$. This may be because the N–NO$_2$ functional group introduces an N–N bond more than C–NO$_2$, which can effectively increase the energy of the compound and increase the sensitivity of the compound. When the D series contains one –NO$_2$, in compounds with $h_{50} > 241$ cm, the h_{50} value is greater when –NO$_2$ is substituted at the C position of the triazole ring (D7–D13, D78–D122), which may be because –NO$_2$ forms an intramolecular hydrogen bond with H at the N position of the triazole ring, thus reducing the sensitivity of compounds. When the D series contains two –NO$_2$ groups, the derivatives are D152–D175 and D251–D427, and the –NO$_2$ of a compound with $h_{50} \geq 297$ cm is substituted on carbon (D152–D175, D259, D263, D290, D299, D301, D302, D306, D307, D358, D365, D370, D372, D375, D416). It indicates that the h_{50} value substituted by –NO$_2$ on C atom is higher than the h_{50} value substituted by –NO$_2$ on N atom. When the D series contains three –NO$_2$ groups, the derivatives are D176–D182 and D428vD558, and the –NO$_2$ of a compound whose h_{50} value is higher than that of TNT is substituted on carbon (D176–D182). It can be seen that C–NO$_2$ has lower energy and is more stable than N–NO$_2$. The relationship between h_{50} and the substitution site of the B and D series is shown in Fig. 5. As can be seen from the figure, in series B, when –NO$_2$ is substituted at R$_1$ or R$_4$ (on C atom), the compound has a higher h_{50} value and lower sensitivity. In the D series, the compound has a higher h_{50} value and the compound is more stable when –NO$_2$ is substituted at R$_2$ or R$_3$ or R$_6$ (on C atom). These are mutually confirmed with the above laws, and
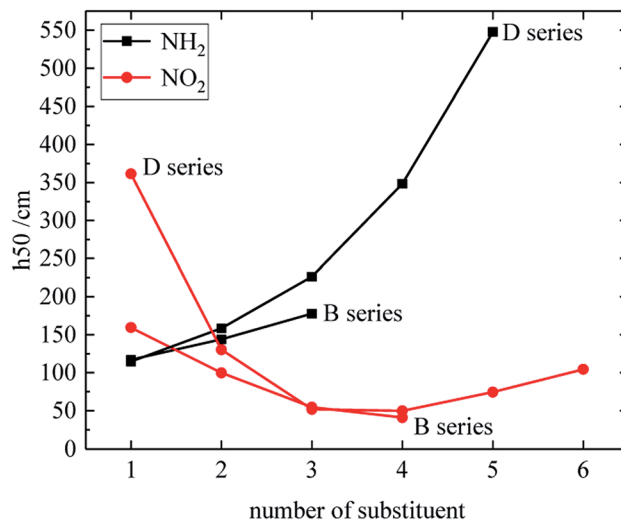
the introduction of –NH$_2$ is more advantageous for the reduction of sensitivity.

The relationship between the h_{50} of B and D series and substituent number is shown in Fig. 6, and the effect of different energetic groups on h_{50} is that –NH$_2$ is more favorable to increase the h_{50} value, which can reduce the sensitivity, and the h_{50} value of the B and D series increases as the substituent number of –NH$_2$ increases. The h_{50} value of the B series decreases as the number of –NO$_2$ groups increases, and the h_{50} value of the D series decreases first as the number of –NO$_2$ groups increases, and then slightly rises. Table 3 shows that the h_{50} value of the A and C series decreases as the number of –NO$_2$ increases. In general, the sensitivity of the compound increases with the number of –NO$_2$, because the introduction of –NO$_2$ enhances the steric hindrance effect or increases the energy. It is also found from Fig. 6 that the derivatives of B and D series has high h_{50} values and low sensitivities when the number of –NO$_2$ is 1. It indicates that when the number of substituents of
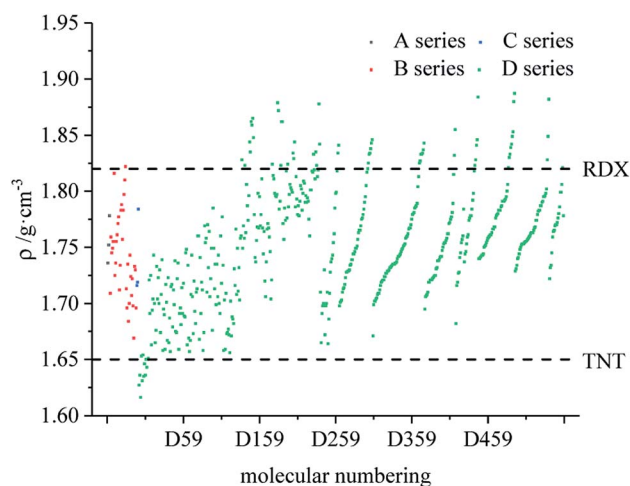

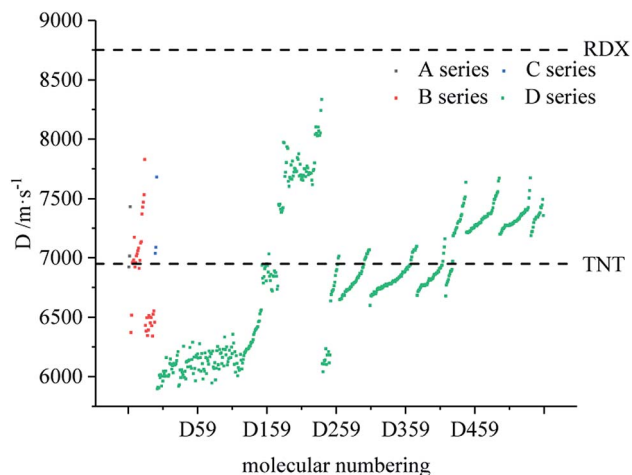**Fig. 7** Comparison of the density of each series of bis-azole derivatives.

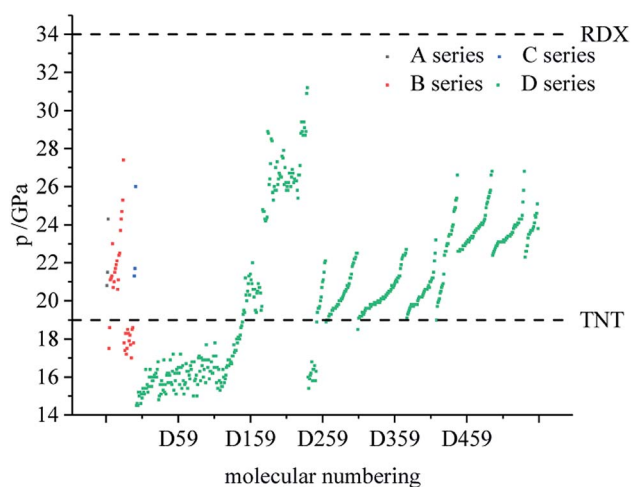Fig. 8 Comparison of the velocity of each series of bis-azole derivatives.

Fig. 9 Comparison of the pressure of each series of bis-azole derivatives.

–NO$_2$ is small, the superconjugation of –NO$_2$ can stabilize the molecular skeleton.

3.3 Predicted density and detonation properties

Fig. 7–9 compare the density, detonation velocity and pressure of all derivatives. There are compounds with higher density than that of RDX in the B and D series, and the detonation performance of the D series is closer to RDX. Compared to the A series, the density and detonation performance of the B series are improved, indicating that the skeleton of the B series is better. From the perspective of density and detonation performance, the application prospects of B and D series are better. D230, D233, D237 and D238 have high detonation velocity (8102, 8101, 8242 and 8335 m s^{-1}) because they have a large density and positive HOF. A large amount of heat is released during detonation, and more heat energy is converted into detonation energy, resulting in a high detonation velocity. In each series, the compounds with lower density compared to TNT are mostly planar molecules, while those with higher density compared to RDX exhibit non-planar structures.

Table 4 lists the density and detonation parameters of partial derivatives, and the density, detonation velocity and pressure of all derivatives of B and D series are listed (see Tables S2 and S5 in ESI†). When the B series contains three –NO$_2$ groups, the density, detonation velocity and pressure of each compound are: B17 < B18 < B19 < B20. The high density and detonation performance values of B19 and B20 indicate that the group density of N–NO$_2$ is larger, thereby increasing the compound density and detonation performance. When the B series substituents are two –NO$_2$ and two –NH$_2$, the density and detonation performance value of each compound increases in the order of B13, B14, B15 and B16, and the distance between –NO$_2$ decreases in this order. It indicates that the energy of the compound increases with the decrease of the distance between –NO$_2$ in the isomer. When the D series contains one –NO$_2$, the

Table 4 Calculated density (ρ) and detonation properties (D, p) of each series of bis-azole derivatives[a]

Comp.	ρ	D	p	Comp.	ρ	D	p	Comp.	ρ	D	p
A1	1.736	6923	20.8	B16	1.788	7137	22.5	D121	1.702	6187	16.4
A2	1.752	7015	21.5	B17	1.757	7370	23.7	D122	1.671	6138	16
A3	1.778	7432	24.3	B18	1.783	7429	24.3	D123	1.688	6065	15.7
B1	1.709	6373	17.5	B19	1.797	7470	24.7	D124	1.686	6114	15.9
B2	1.759	6518	18.6	B20	1.81	7532	25.3	D125	1.682	6144	16.1
B3	1.745	6957	21.1	B21	1.822	7827	27.4	D146	1.844	6421	18.6
B4	1.749	6969	21.2	C1	1.716	7038	21.3	D147	1.835	6463	18.7
B5	1.755	6982	21.3	C2	1.719	7089	21.7	D148	1.862	6469	18.9
B6	1.816	7174	23	C3	1.784	7679	26	D152	1.779	6938	21.2
B7	1.725	6924	20.7	D6	1.654	6017	15.2	D153	1.741	6828	20.3
B8	1.736	6960	21	D7	1.635	5919	14.6	D154	1.737	6787	20
B9	1.755	7016	21.5	D8	1.646	6003	15.1	D176	1.824	7451	24.8
B10	1.761	7034	21.7	D31	1.739	6210	16.8	D177	1.814	7442	24.7
B11	1.771	7060	21.9	D32	1.658	5918	14.8	D178	1.811	7455	24.7
B12	1.777	7082	22.1	D33	1.695	5930	15	D183	1.879	7973	28.9
B13	1.712	6911	20.6	D34	1.69	6055	15.6	D237	1.878	8242	30.9
B14	1.734	6977	21.1	D35	1.659	5991	15.1	D238	1.842	8335	31.2
B15	1.783	7124	22.4	D120	1.656	6060	15.5				

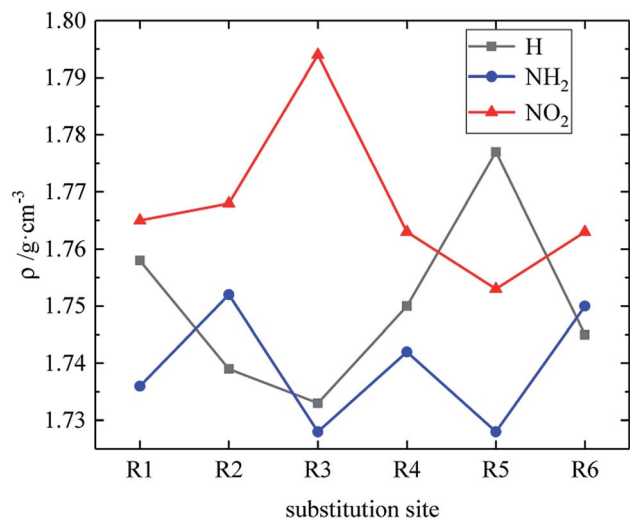[a] ρ (g cm^{-3}), D (m s^{-1}), p (GPa).

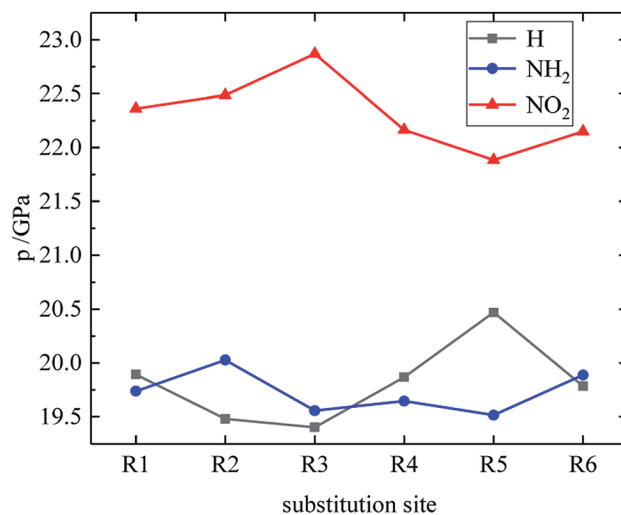**Fig. 10** The relationship between the density and substitution sites (D series).

Fig. 12 The relationship between the detonation pressure and substitution sites (D series).

derivatives are D1–D151 and D239–D250, and the density range is 1.616–1.865 g cm^{-3}. The density of the compounds where the substitution site of –NO$_2$ are at the diazole ring is all greater than that of TNT (1.65 g cm^{-3}), including compounds D15–D23, D25, D27–D31, D34, D36, D39, D43, D44, D47, D48, D50–D52, D54, D57, D58 and D123–D151. When the D series contains one –NO$_2$ group, the –NO$_2$ of compounds having a density greater than that of RDX is substituted at R$_3$, and the –NO$_2$ group of compounds having a higher detonation velocity and pressure is also basically substituted at R$_3$, which is the case for compounds D146–D151. In the four series, the compounds whose density is less than or equal to the density of TNT are the D series (D1–D3, D5 and D7–D12), which contain one –NO$_2$ group substituted at the triazole ring. The relationship between density, detonation velocity and detonation pressure of the D series and substitution site is shown in Fig. 10–12: when R$_3$ is
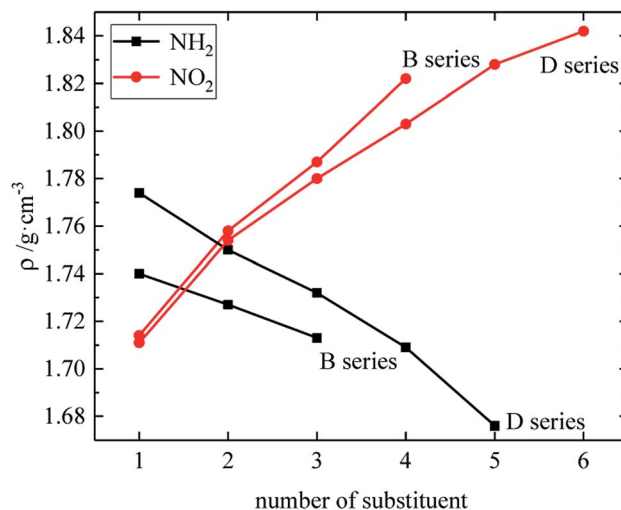

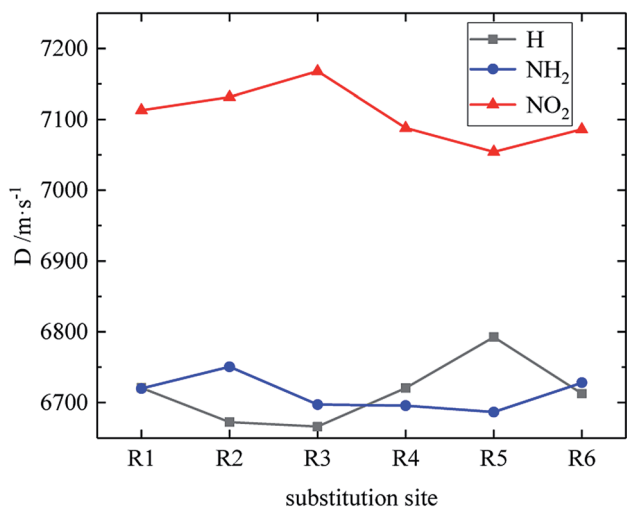**Fig. 13** The relationship between the density and number of substituent (B, D series).

–NO$_2$, it contributes the most to the density, detonation velocity and detonation pressure, and it's mutually confirmed with the above-mentioned regular phenomenon. In addition, –NO$_2$ contributes to the density and detonation performance to a greater extent than –NH$_2$.

The relationship between the density, detonation performance and the substituent number of B and D series is shown in Fig. 13–15. The relationship between the contributions of different energetic groups to the density and detonation performance is –NO$_2$ > –NH$_2$. The density, detonation velocity and pressure of B and D series decrease as the number of –NH$_2$ increases, and increase as the number of –NO$_2$ increases, which supports the viewpoint that the introduction of more –NO$_2$ groups in the molecule can improve the detonation performance. Table 4 shows that the density and detonation performance of A and C series improve as the number of –NO$_2$

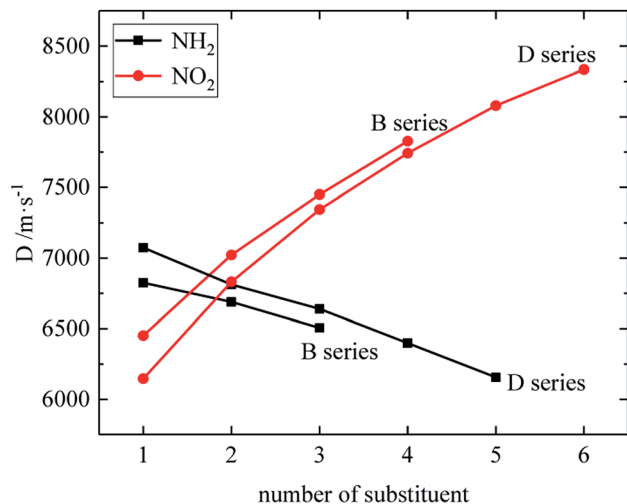**Fig. 11** The relationship between the detonation velocity and substitution sites (D series).
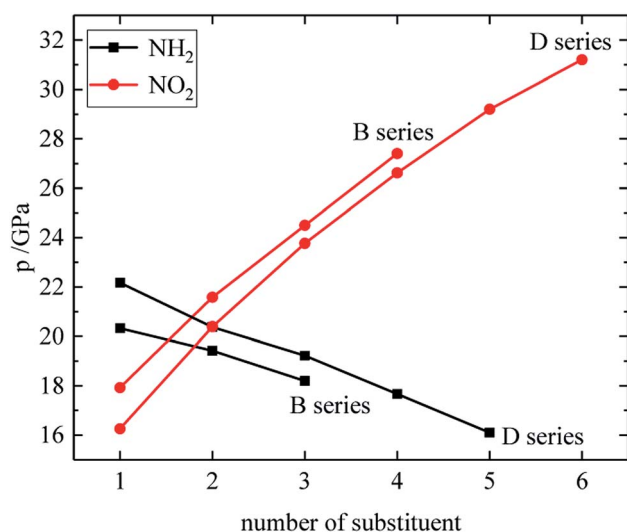
Fig. 14 The relationship between the detonation velocity and number of substituent (B, D series).

Fig. 15 The relationship between the detonation pressure and number of substituent (B, D series).

Fig. 16 Calculated Q_{NO_2}, ρ, D, p of derivatives.

increases, and among all derivatives, each compound in which all substituents are –NO_2 has the highest density (except D238), detonation velocity and detonation pressure in the corresponding respective series of derivatives.

3.4 Predicted potential HEDM candidates

The ideal HEDM candidates should be stable and exhibit effective detonation performance, and of the various factors that constrain each other need to be considered.[51] It is generally believed that the promising HEDC meets the following requirements: $\rho > 1.9$ g cm^{-3}, $D > 9.0$ km s^{-1} and $p > 40$ GPa.[52] The HEDM candidates have potential for further development, prompting further investigation into compound synthesis. Compounds meeting the following conditions are selected from each series, and the detonation performance and other
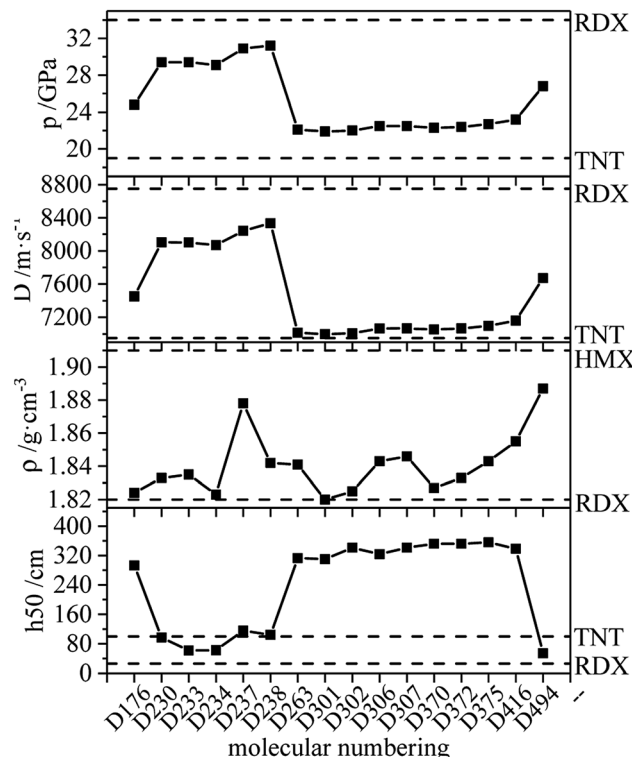
parameters are shown in Fig. 16: (1) $\rho \geq \rho$ (RDX), $D > D$ (TNT), $p > p$ (TNT), $-Q_{NO_2} \geq -Q_{NO_2}$ (RDX); (2) $\rho \geq \rho$ (RDX), $D \geq 8000$ m s^{-1}; (3) ρ is the largest.

According to the figure, the variation trend of detonation velocity and detonation pressure is the same, while this trend differs from that of density. This indicates that the density is not the only parameter that determines detonation velocity and pressure, and the detonation heat also affects the detonation performance. The density of the compound in the figure is greater than or equal to that of RDX (1.82 g cm^{-3} (ref. 53)). Also, the unique nitrogen heterocycle of D494 increases the density, and its density is the largest at 1.887 g cm^{-3}, which is close to the density of HMX (1.91 g cm^{-3} (ref. 53)). D238 has the highest detonation velocity (8335 m s^{-1}) and detonation pressure (31.2 GPa), which are close to RDX (8750 m s^{-1}, 34 GPa (ref. 53)). Meanwhile, the h_{50} value of D176 is larger than that of TNT, indicating that D176 appears to be insensitive, which is mainly due to the intramolecular hydrogen bond. Calculations revealed that D230, D233, D234, D237 and D238 exhibit high detonation performances and might be HEDM candidates, and the group density of N–NO_2 in those molecules is relatively high, which increases the molecular characteristic density and the crystal density of explosives and thus increases the detonation velocity. In addition, the increase in the number of detonating groups, the existence of the unique nitrogen heterocycle structure and the ring tension lead to large detonation velocity, detonation pressure and high energy.

Consequently, based on the results of detonation properties and stability, compounds D176 (1.824 g cm^{-3}, 7451 m s^{-1},

24.8 GPa, 293 cm), D230 (1.833 g cm^{-3}, 8102 m s^{-1}, 29.4 GPa, 97 cm), D233 (1.835 g cm^{-3}, 8101 m s^{-1}, 29.4 GPa, 62 cm), D234 (1.823 g cm^{-3}, 8068 m s^{-1}, 29.1 GPa, 62 cm), D237 (1.878 g cm^{-3}, 8242 m s^{-1}, 30.9 GPa, 116 cm), D238 (1.842 g cm^{-3}, 8335 m s^{-1}, 31.2 GPa, 104 cm) and D494 (1.887 g cm^{-3}, 7670 m s^{-1}, 26.8 GPa, 54 cm) can be considered as potential HEDM candidates.

4 Conclusions

Based on DFT calculation, the density, heat of formation, detonation velocity, detonation pressure and h_{50} values of derivatives were compared, and the relationship between structure and performance was studied. The performance parameters are affected by the molecular structure, and the type and number of groups in the structure, the arrangement of the groups and the intramolecular symmetry appear to be influential parameters. The conclusions are as follows: (1) compared with the A series, the B series has higher density, higher heat of formation, better detonation performance and better stability, indicating that the energy improves with the increase of the nitrogen content, and the skeleton of B series is better. (2) The density, heat of formation, detonation velocity and detonation pressure of the compound improve with the increase in the number of the –NO$_2$ group. However, the variation trend of the h_{50} value is opposite. (3) The density, detonation velocity and detonation pressure of the compound decrease as the number of the –NH$_2$ group increases, while the heat of formation and h_{50} value increase as the number of the –NH$_2$ group increases, and the growth rate of heat of formation here is less than the growth rate of heat of formation in which the substituent is –NO$_2$. (4) The h_{50} value indicates that the molecular stability decreases as the number of the –NO$_2$ group increases; however, if the substituent is –NH$_2$, the opposite is true. (5) –NO$_2$ substituents are advantageous for increasing density, heat of formation and detonation properties, while –NH$_2$ substituents are advantageous for increasing stability. (6) The presence of multiple nitrogen–nitro groups (N–NO$_2$) can effectively improve oxygen balance, so these compounds generally have high density and low sensitivity. (7) In terms of detonation performance and stability, compounds D176, D230, D233, D234, D237, D238 and D494 yield promising results and may be considered as potential HEDM candidates.

Conflicts of interest

There are no conflicts to declare.

Acknowledgements

References

1 Y. J. Shu and J. C. Huo, *Theory of Explosives*, Chemical Industry Press, Beijing, 2011, pp. 288–310.

2 X. J. Wang, K. Z. Xu, Q. Sun, B. Z. Wang, C. Zhou and F. L. Zhao, *Propellants, Explos., Pyrotech.*, 2015, **40**(1), 9–12.

3 P. He, H. Mei, J. Yang, *et al.*, Design and properties of a new family of bridged bis (nitraminotetrazoles) as promising energetic materials, *New J. Chem.*, 2019, **43**(10), 4235–4241.

4 G. Y. Hang, W. L. Yu, T. Wang, *et al.*, Theoretical investigations on stabilities, sensitivity, energetic performance and mechanical properties of CL-20/NTO cocrystal explosives by molecular dynamics simulation, *Theor. Chem. Acc.*, 2018, **137**(8), 114.

5 X. J. Zhang, Y. C. Li, W. Liu, Y. Z. Yang, L. Peng and S. P. Pang, *Chin. J. Energ. Mater.*, 2012, **20**(4), 491–500.

6 X. L. Xia, *Molecular designs of new energetic nitrogen-containing heterocycle compounds*, Nanjing University of Science & Technology, Nanjing, 2013.

7 Z. M. Li, J. G. Zhang, T. L. Zhang and Y. J. Shu, *Prog. Chem.*, 2010, **22**(4), 639–647.

8 Y. N. Li, T. Tang, P. Lian, Y. F. Luo, W. Yang, Y. B. Wang, H. Li, Z. Z. Zhang and B. Z. Wang, *Chin. J. Org. Chem.*, 2012, **32**(3), 580–588.

9 Q. H. Zhang and J. M. Shreeve, *Angew. Chem., Int. Ed.*, 2013, **52**(34), 8792–8794.

10 L. Guanqiong, L. Yuchuan, M. Qiaoli, *et al.*, Research Progress in Synthesis of Nitrogen-Rich Zole-Ring Compounds by Cycloaddition Reaction, *Chin. J. Org. Chem.*, 2010, **30**(10), 1431–1440.

11 W. Wang, G. Cheng, H. Xiong, *et al.*, Functionalization of fluorodinitroethylamino derivatives based on azole: a new family of insensitive energetic materials, *New J. Chem.*, 2018, **42**(4), 2994–3000.

12 X. C. Huang, Z. J. Wang, T. Guo, *et al.*, Review on Energetic Compounds Based on 1, 2, 4-Oxadiazoles, *Chin. J. Energ. Mater.*, 2017, **25**, 603–611.

13 J. L. Zhang, F. Q. Bi, B. Z. Wang, *et al.*, Review on the Aza-polyaromatic Ring Energetic Compounds, *Chin. J. Energ. Mater.*, 2016, **24**(8), 810–819.

14 B. M. Rice and J. Hare, *Thermochim. Acta*, 2002, **384**(1), 377–391.

15 H. Muthurajan, R. Sivabalan, M. B. Talawar, M. Anniyappan and S. Venugopalan, *J. Hazard. Mater.*, 2006, **133**(1—3), 30–45.

16 C. Adachi, T. Tsutsui and S. Saito, *Appl. Phys. Lett.*, 1989, **55**(15), 1489–1491.

17 H. X. Gao and J. M. Shreeve, *Chem. Rev.*, 2011, **111**(11), 7377–7436.

18 A. A. Korkin and R. J. Bartlett, *J. Am. Chem. Soc.*, 1996, **118**(48), 12244–12245.

19 P. Hohenberg and W. Kohn, *Phys. Rev.*, 1964, **136**(3B), B864–B871.

20 W. Kohn and L. J. Sham, *Phys. Rev.*, 1965, **140**(4A), A1133–A1138.

21 R. G. Parr and W. T. Yang, *Density-functional theory of atoms and molecules*, Oxford University Press, New York, 1989, pp. 1–333.

22 X. J. Xu, W. H. Zhu and H. M. Xiao, *J. Phys. Chem. B*, 2007, **111**(8), 2090–2097.

23 G. X. Wang, H. M. Xiao, X. H. Ju and X. D. Gong, *Propellants, Explos., Pyrotech.*, 2006, **31**(5), 361–368.

24 X. J. Xu, H. M. Xiao, X. H. Ju and X. D. Gong, *Chin. J. Org. Chem.*, 2005, **25**(5), 536–539.

25 L. M. Qiu, X. D. Gong, J. Zheng and H. M. Xiao, *Chin. J. Energ. Mater.*, 2008, **16**(6), 647–651, 668.

26 Y. Zhou, X. P. Long and Y. J. Shu, *J. Mol. Model.*, 2010, **16**(5), 1021–1027.

27 Y. Pan, W. H. Zhu and H. M. Xiao, *Struct. Chem.*, 2013, **24**(4), 1071–1087.

28 F. Wang, G. X. Wang, H. C. Du, J. Y. Zhang and X. D. Gong, *J. Phys. Chem. A*, 2011, **115**(47), 13858–13864.

29 B. M. Rice and E. F. Byrd, *J. Mater. Res.*, 2006, **21**, 2444–2452.

30 Z. Yu and E. R. Bernstein, *J. Phys. Chem. A*, 2013, **117**, 10889–10902.

31 C. Cao and S. Gao, *J. Phys. Chem. B*, 2007, **111**, 12399–12402.

32 Q. Wu, Q. Li, G. Yan, *et al.*, Molecular design of novel super high energy compounds by incorporating the difluoramino group, N-oxide and different bridge groups into the 1H-tetrazole, *J. Fluorine Chem.*, 2019, **218**, 21–26.

33 A. Nirwan, A. Devi and V. D. Ghule, Assessment of density prediction methods based on molecular surface electrostatic potential, *J. Mol. Model.*, 2018, **24**(7), 166.

34 P. Politzer, J. Martinez, J. S. Murray, *et al.*, An electrostatic interaction correction for improved crystal density prediction, *Mol. Phys.*, 2009, **107**(19), 2095–2101.

35 L. Qiu, H. M. Xiao, X. H. Ju and X. D. Gong, *Acta Chim. Sin.*, 2005, **63**(5), 377–384.

36 M. H. Lin, *Computational methods and applications of quantum chemistry*, Science Press, Beijing, 2004, pp. 227–233.

37 B. M. Rice, J. J. Hare and E. F. C. Byrd, *J. Phys. Chem. A*, 2007, **111**(42), 10874–10879.

38 Sobereva, *Use Multiwfn to predict properties such as crystal density, evaporation enthalpy, boiling point, and free energy of dissolution[EB/OL]*, 2016-6-21, http://sobereva.com/337.

39 T. Lu and F. Chen, Multiwfn: a multifunctional wavefunction analyzer, *J. Comput. Chem.*, 2012, **33**(5), 580–592.

40 J. Y. Zhang, F. Wang and X. D. Gong, *Struct. Chem.*, 2013, **24**(4), 1339–1346.

41 M. J. Kamlet and S. J. Jacobs, *J. Chem. Phys.*, 1968, **48**(1), 23–35.

42 T. Wei, W. H. Zhu, X. W. Zhang, Y. F. Li and H. M. Xiao, *J. Phys. Chem. A*, 2009, **113**(33), 9404–9412.

43 T. Wei, W. H. Zhu, J. J. Zhang and H. M. Xiao, *J. Hazard. Mater.*, 2010, **179**(1—3), 581–590.

44 L. Türker, T. Atalar, S. Gümüş and Y. Çamur, *J. Hazard. Mater.*, 2009, **167**(1—3), 440–448.

45 J. C. Gálvez-Ruiz, G. Holl, K. Karaghiosoff, T. M. Klapötke, K. Löhnwitz, P. Mayer, H. Nöth, K. Polborn, C. J. Rohbogner, M. Suter and J. J. Weigand, *Inorg. Chem.*, 2005, **44**(12), 4237–4253.

46 M. J. Frisch, G. W. Trucks, H. B. Schlegel, *et al.*, *Gaussian 09, Revision B.01*, Gaussian, Inc., Wallingford, 2009.

47 M. H. V. Huynh, M. A. Hiskey and C. J. Pollard, *Chin. J. Energ. Mater.*, 2004, **22**(4), 217–229.

48 M. H. V. Huynh, M. A. Hiskey, J. G. Archuleta, E. L. Roemer and R. Gilardi, *Angew. Chem., Int. Ed.*, 2004, **43**(42), 5658–5661.

49 M. Tian, W. J. Chi, Q. S. Li, *et al.*, Theoretical design of highly energetic poly-nitro cage compounds, *RSC Adv.*, 2016, **6**(53), 47607–47615.

50 Y. Y. Guo, W. J. Chi, Z. S. Li, *et al.*, Molecular design of N–NO2 substituted cycloalkanes derivatives Cm(N–NO2)m for energetic materials with high detonation performance and low impact sensitivity, *RSC Adv.*, 2015, **5**(48), 38048–38055.

51 X. J. Xu, H. M. Xiao, X. D. Gong, X. H. Ju and Z. X. Chen, *J. Phys. Chem. A*, 2005, **109**(49), 11268–11274.

52 L. Qiu, *Molecular Design of High Energy Density Materials (HEDM)—Cyclic Nitramines*, Nanjing University of Science and Technology, Nanjing, 2007.

53 M. B. Talawar, R. Sivabalan, T. Mukundan, H. Muthurajan, A. K. Sikder, B. R. Gandhe and R. A. Subhananda., *J. Hazard. Mater.*, 2009, **161**(2–3), 589–607.